Seasonal climate summary southern hemisphere (spring 2003): neutral conditions remain in the tropical Pacific, but dry conditions dominate northeast Australia

Andrew B. Watkins
National Climate Centre, Bureau of Meteorology , Australia

(Manuscript received August 2004)

Atmospheric and oceanic conditions in the southern hemisphere are reviewed for the 2003 austral spring season. Particular emphasis is given to the Australian and Pacific regions. The 2002-03 El Niño event ended in autumn, with conditions remaining neutral during winter and then through spring. The neutral spring El Niño-Southern Oscillation (ENSO) state remained, despite equatorial ocean surface and sub-surface temperature anomalies in the tropical Pacific increasing slightly during the season. Convection, however, was confined to the western tropical Pacific, suggesting that the slightly warmer than normal oceanic conditions failed to significantly couple with the atmosphere. At the high latitudes, the Antarctic ozone hole reached 28 million km^2, a maximum size comparable to the record area observed in 2000. Over Australia, the neutral ENSO conditions failed to bring even average rainfall to a significant portion of the eastern half of the continent, with only below average rainfall totals for large areas of Queensland and the Northern Territory, as well as parts of northern and central New South Wales. Both maximum and minimum temperatures were generally above average in the north and east of the country, whilst in the south temperatures were cooler than average.

Introduction

After the demise of the El Niño in the equatorial Pacific during autumn (Beard 2004), neutral conditions remained through the winter (Dawkins 2004) and subsequent spring. The neutral state was typified by the Southern Oscillation Index (SOI), which averaged only –2.5 over the season, and the Multivariate ENSO Index (MEI), which came in with a ranking of 37 out of 54 years. Trade winds were generally near normal, whilst sea-surface and subsurface temperature anomalies along the equator rose slightly during the course of the season. As a result of this warming, the Niño 4 index reached greater than one standard deviation above the mean during both October and November. In some contrast, over the central to eastern Pacific, high cloud amounts were suppressed. Only two weak Madden-Julian Oscillation (MJO)

Corresponding author address: Andrew B. Watkins, National Climate Centre, Bureau of Meteorology, GPO Box 1289K, Melbourne, Vic. 3001, Australia.
Email: a.watkins@bom.gov.au

(Madden and Julian 1971, 1972) events occurred during the season, with neither having any long-term impact upon the atmospheric or oceanic state.

In the mid-latitudes, the low-level westerlies tended to be further south than normal, suggesting a possible southwards shift in the subtropical ridge of high pressure.

At the higher latitudes, the springtime hole in the ozone layer reached a size of 28 million km^2, comparable to the record ozone hole recorded in 2002 and far exceeding the mean 1991-2002 peak value of 21 million km^2. The area of ozone values which had a total column ozone 50 per cent or less of their pre-ozone hole (1964-76) mean value reached 18 million km^2, the first time the sub-fifty per cent area had reached 15 million km^2 and only the fourth time it had exceeded 10 million km^2.

Over Australia, rainfall patterns showed above average rainfall over much of Western Australia, and below average rainfall over Queensland and the Northern Territory. Some lowest on record totals were recorded in far north Queensland. The remainder of the continent experienced closer to average rainfall. Maximum temperature anomalies displayed warmer than normal conditions over much of Queensland and the Northern Territory, whilst cooler than normal maximum temperatures were experienced along Australia's southern coast and through much of Tasmania and Victoria. Similarly, minimum temperatures were above normal over parts of Queensland and the Northern Territory, but were cooler than normal over much of the southeast of the continent, including parts of New South Wales and Victoria.

Data

The main sources of information used for this summary were the *Climate Monitoring Bulletin* (Bureau of Meteorology, Melbourne, Australia) and the *Climate Diagnostics Bulletin* (Climate Prediction Center, Washington D.C., USA). Data sources are given in the Appendix.

Pacific Basin climate indices

The Southern Oscillation Index (SOI)*

The neutral values of the Troup Southern Oscillation Index (SOI) during the austral winter of 2003 (Dawkins 2004) were maintained through the spring. September, October and November 2003 SOI values were –2.2, –1.9 and –3.4 respectively, resulting in a mean spring value of the SOI of –2.5 (Fig. 1). Throughout the season, SOI values were always within one standard deviation of the mean (the Troup SOI has a standard deviation of 10) as were the raw Tahiti minus Darwin values, from which the SOI is based.

Fig. 1 Southern Oscillation Index, January 1999 to November 2003 inclusive. Means and standard deviations based on the period 1933-92.

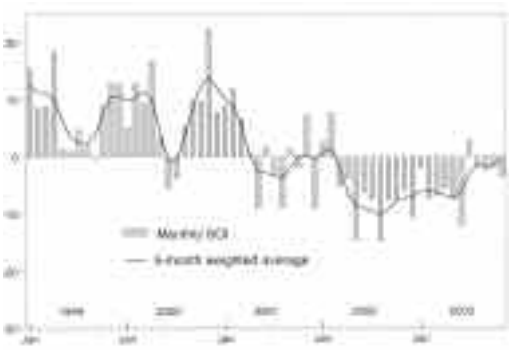

Mean sea-level pressure (MSLP) anomalies at Tahiti and Darwin generally remained close to their long-term mean during the season. At Darwin, the November deviation of +0.6 hPa above the long-term mean was the largest monthly anomaly for either station during the season.

The neutral state of the tropical atmosphere suggested by the SOI was supported by the values of the Climate Diagnostics Center (CDC) Multivariate ENSO Index (MEI) (Wolter and Timlin 1993, 1998), an index derived from a number of atmospheric and oceanic parameters typically associated with El Niño and La Niña, with negative values indicating cooler conditions and positive values indicating warmer conditions. The MEI values during the season had rankings of 37 (out of 54 years); a rise in rankings from those observed during winter (28 and 32). An MEI ranking of 44 to 54 is considered to be an El Niño event.

Outgoing long wave radiation

The time series from January 1999 to November 2003 of monthly standardised outgoing long wave radiation (OLR) anomalies for the region from 5ºN to 5ºS, 160ºE to 160ºW, is shown in Fig. 2. These data were provided by the Climate Prediction Center, Washington D.C. (CPC 2003). Negative (positive) values of the OLR index suggest cooler (warmer) black-body temperatures, which tend to be associated with an increase (decrease) in high cloud amount. (This may also signal increased rainfall.) Studies have

*The SOI used here is ten times the monthly anomaly of the difference in mean sea-level pressure between Tahiti and Darwin, divided by the standard deviation of that difference for the relevant month, based on the period 1933-1992.

Fig. 2 **Standardised anomaly of monthly outgoing long wave radiation averaged over 5°N-5°S and 160°E-160°W, for January 1999 to November 2003. Negative (positive) anomalies indicate enhanced (reduced) convection and rainfall. Anomalies are based on a 1979-95 base period. After CPC (2003).**

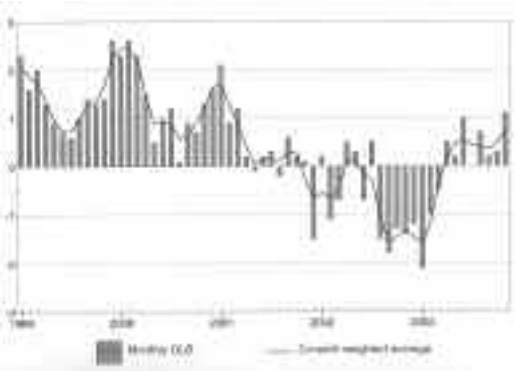

shown that during El Niño events, OLR is generally reduced (i.e. convection is generally enhanced) along the equator, particularly near and east of the date-line. During La Niña events, OLR is often increased (i.e. convection is often suppressed) over the same region (Hoerling et al. (1997), Vincent et al. (1998)).

The standardised OLR anomaly for a box centred on the date-line is shown in Fig. 2. During the individual months of spring 2003 the OLR anomaly for this region rose from +0.2 in September to +0.3 in October, before rising sharply by almost one standard deviation to +1.1 in November, indicating a suppression of convection in the central equatorial Pacific late in the year.

The OLR values for spring 2003 were in marked contrast to the values observed during the spring of 2002 (–1.8, –1.3 and –1.4 for September, October and November respectively (Watkins 2003)), when the El Niño event was approaching its December peak.

Figure 3 shows the spatial pattern of OLR anomalies observed during the season. This shows that the region of increased OLR (suppressed convection) extended far beyond the boundaries of the region close to the date-line. The area of suppressed convection extended east to near the South American coast, whilst in the far western equatorial Pacific, decreased OLR (increased convection) was apparent. This pattern is arguably more reminiscent of cool ENSO conditions.

Unlike 2002, when substantial active phases of the MJO entered the western equatorial Pacific in late August and November (Watkins 2003), spring 2003 saw only relatively weak MJO activity in August/September and again in October. Both events failed to have any long-term significant impact upon atmospheric or oceanic conditions, with only some slight slackening of the trade winds in early September and a period of westerly anomalies in late October/early November. These latter westerly anomalies triggered a weak downwelling oceanic Kelvin wave, however this failed to produce any long-term warming in the subsurface or at the surface. (This is discussed further in the following section.)

The overall pattern of OLR for the South Pacific region saw increased OLR (decreased high cloud) over much of the South Pacific (Fig. 3), which was reflected in the rainfall anomalies (not shown) which were generally below average: by November, Fiji had experienced its fifth month in a row of below average rainfall. The South Pacific convergence zone (SPCZ) was generally south to southwest of its climatological position. (During warm ENSO periods the SPCZ is ordinarily north and east of its average position, while during cool events it tends to be shifted south and west (Vincent 1993).) Despite this shift, the SPCZ was generally weak, the exception being in the vicinity of the Solomon Islands during November.

Over Australia (not shown), OLR anomaly values for the season were positive over much of the country, with largest values (12 to 17 W m^{-2}) in eastern Queensland.

Ocean patterns

Sea-surface temperatures

Despite the neutral state of the equatorial atmosphere, the spring 2003 sea-surface temperature (SST) anomaly distribution (Fig. 4) displayed weakly positive

Fig. 3 **Anomalies of outgoing long wave radiation for spring 2003 (W m^{-2}), based on a base period of 1979-98.**

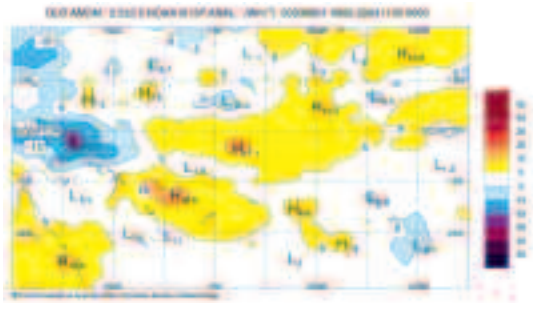

Fig. 4 Anomalies of sea-surface temperature for spring 2003 (°C).

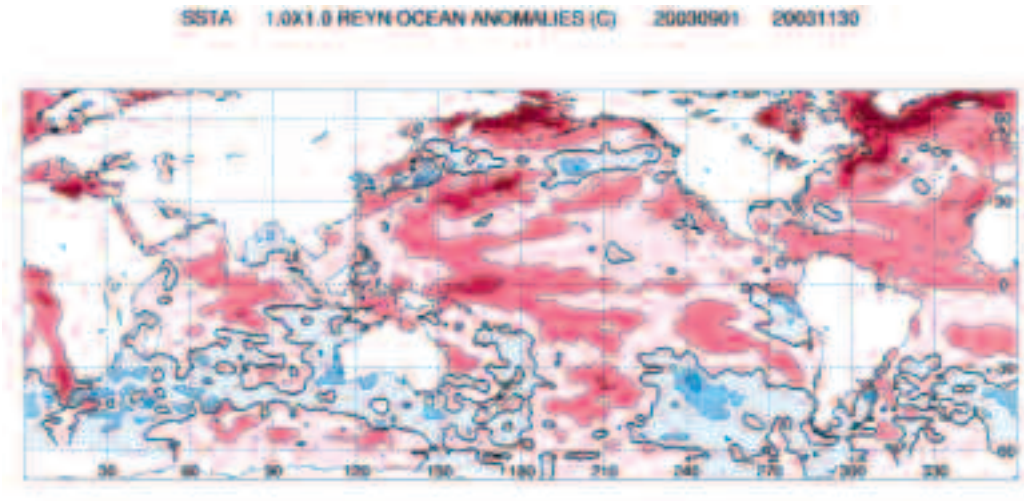

anomalies along the equator from Indonesia to near 100°W, less than 20° of longitude from the South American coast. However, despite this widespread warm signal, the magnitudes of the SST anomalies were small, with values generally less than 1°C. Largest seasonal anomalies occurred in the western Pacific warm pool region, west of the date-line, where values exceeded +1°C.

The seasonal SST anomalies along the equator were a reflection of a fairly consistent pattern across the individual months. A weak warming in the central to western equatorial Pacific occurred during September as trade winds relaxed in response to an active (but weak) phase of the MJO during late August/early September. A second active MJO in late October/early November brought stronger westerly wind anomalies to the western Pacific which triggered a downwelling oceanic Kelvin wave. Whilst this effectively warmed the subsurface, the westerly wind anomalies also brought about localised warming of the surface through a reduction in the upwelling of deeper waters. This reduced upwelling brought SST anomalies of above +1°C to a broad region, from near 160°E to 160°W, during November.

In some contrast to this slightly warm SST anomaly pattern in the central and western equatorial Pacific, cool anomalies were present in the far east, near the South American coast during September, but these gradually weakened during the season as earlier Kelvin waves reached the eastern boundary.

The increasing trend in the central and western equatorial Pacific SST anomalies, as well as the weakening of anomalies closer to the South American coast, were evident in the values for the various Niño indices. In the eastern equatorial Pacific, the Niño 1 and 2 values for September of –0.82°C and –0.15°C, respectively, rose to –0.04°C and +0.88°C by November. Similarly, in the central equatorial Pacific the Niño 3, 3.4 and 4 values rose from +0.26°C, +0.53°C and +0.78°C in September to +0.57°C, +0.69°C and +1.11°C in November. The Niño 4 region was above one standard deviation from the mean for both October and November (the October and November standard deviations for Niño 4 are 0.72°C and 0.80°C respectively.) It is interesting to note that just as in 2002 (Watkins 2003), November later proved to be the peak of the warming in the central equatorial Pacific.

In the mid to high latitudes, SST anomalies were generally negative with values 0.5 to 1.0°C below normal occurring between approximately 30°S and 50°S. This band of anomalous SST values was evident around much of the globe, the only exception being a pool of warmer than usual water (anomalies generally between +0.5°C and +1.0°C) between the date-line and 140°W. This region corresponds to the western half of a large anticyclonic anomaly (see Fig. 8) and hence strong northerly flow in the low levels (Fig. 12), effectively driving warmer waters southwards, as well as advecting warmer than normal air over the water.

At the high latitudes (south of 60°S) SST values were generally within 0.5°C of their long-term mean. However, it is worth noting that spring sees the time of maximum extent in the Antarctic sea-ice pack (Watkins and Simmonds 1999), and hence, in gener-

al, SST anomalies in the vicinity of the Antarctic coast are relatively meaningless (as they are ice covered), or very stable, as SSTs remain near constant at around –1.8ºC (the freezing point of sea water).

Just to the north of the sea-ice edge, between 50°S and 60°S, there were some regions of SST anomalies above +0.5°C. The most notable of these occurred off East Antarctica, south and to the west of Australia. Sea-ice anomalies for this region (not shown) indicate a slightly more northwards sea-ice edge than normal during September, easing to near normal by November. This would ordinarily have been expected to bring slightly lower than normal SST values, due to high sensible and latent heat fluxes north of the sea-ice edge (Watkins and Simmonds 1999).

Overall sea-ice concentration anomalies (not shown) were a mix of decreased concentration north of the Ross Sea, the Weddell Sea and the Amery Ice Shelf, but increased sea-ice concentration off much of East Antarctica and Dronning Maud Land, as well as in the Bellingshausen Sea and parts of the Amundsen Sea. The increased sea-ice edge in the latter two regions relates well to the findings of Yuan and Martinson (2001), who observed lagged correlations in these regions between the latitude of the sea-ice edge in the Amundsen and Bellingshausen Seas and Niño 3 values, with strong correlations occurring six to 12 months after their peak values. Similarly, Kwok and Comiso (2002) showed correlations of between 0.38 and 0.50 in the same region between sea-ice edge anomalies and the SOI at lags of between seven and 11 months. The 2002-03 El Niño event saw peak SST values occur in November-December 2002 (Watkins 2003).

In the Australian region, September to November 2003 SSTs were generally near normal. Anomalies of greater than +0.5°C were apparent off the southern Queensland/northern New South Wales coast, as well as around the Top End (Northern Territory). In contrast, anomalies of below –0.5°C occurred off the southwestern Western Australian coast. Whilst the warm anomalies off the Queensland/New South Wales coasts, and to a lesser degree the Top End, were apparent during the winter (Dawkins 2004), the cool anomalies off Western Australia had emerged during the spring, possibly associated with east to southeast wind anomalies over the region (Fig. 13).

Globally averaged, 2003 austral spring SSTs were 0.52°C above the 1880-2002 mean (NCDC 2004), the second warmest September to November period on record. In the southern hemisphere, oceans were 0.46°C above average; the fifth warmest on record. It is also interesting to note the very high SST values in the high latitudes of the northern hemisphere (Fig. 4), where SST anomalies reached in excess of +3°C in both the North Atlantic and North Pacific.

Subsurface ocean patterns

The Hovmöller diagram for the 20°C isotherm depth anomaly across the equator from January 1995 to November 2003 is shown in Fig. 5. The 20°C isotherm depth is generally situated close to the equatorial ocean thermocline, the region of greatest temperature gradient with depth and the boundary between the warm near surface and cold deep ocean water. Changes in the thermocline depth may act as a precursor to future changes at the surface.

During September and into early October, the equatorial subsurface temperatures were generally near normal in the central and western Pacific. In the east, however, the thermocline was depressed with anomalies of over +20 m, and maxima of +30 m reached at times. This warm anomaly was essentially the remnants of a Kelvin wave that crossed the equatorial Pacific during June and July (Dawkins 2003).

An active phase of the MJO brought westerly wind anomalies to the western equatorial Pacific during mid to late October. The relaxation of the trade winds reduced the Ekman divergence and hence the

Fig. 5 **Time-longitude section of the monthly anomalous depth of the 20°C isotherm at the equator for January 1995 to November 2003. Base period: 1979-89. Contour interval is 10 m.**

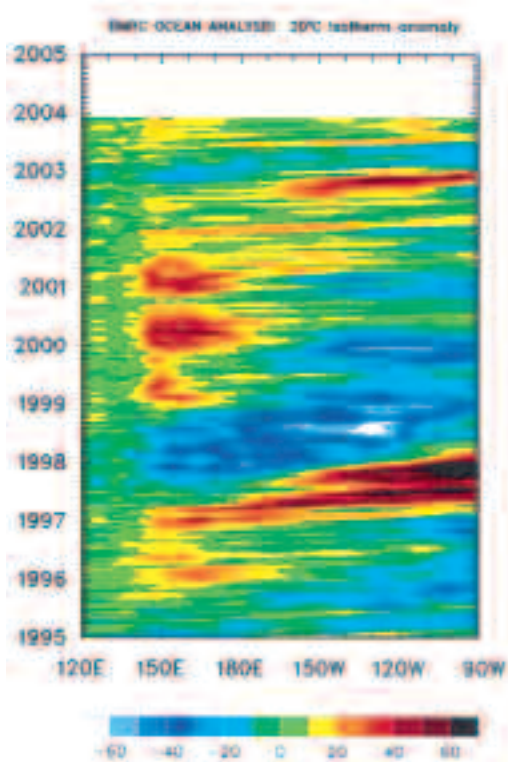

upwelling of deeper cool waters. This effectively deepened the thermocline, thus triggering a downwelling oceanic Kelvin wave along the thermocline. This Kelvin wave crossed the equatorial Pacific during late October, November and early December 2003, but was relatively weak and hence failed to establish truly warm conditions in the central or eastern equatorial Pacific. In fact, some degree of cooling was left in its wake.

The oceanic downwelling Kelvin wave is also shown in the cross section of the equatorial Pacific temperature anomaly profile (Fig. 6), which shows temperatures down to 400 m for the months from August to November 2003. Whilst the temperature profile shows some slightly positive anomalies nearer the surface, (particularly on or west of the date-line; associated with the warm Nino 3, 3.4 and 4 indices), at depths around 150 m (the vicinity of the thermocline in the central to western Pacific) cool anomalies were apparent during September, with values as low as –2.5°C. However, these cool anomalies were eroded somewhat by the Kelvin wave during October and November. As a result, November thermocline anomalies were generally only of the order of –1°C, a decrease of 1 to 1.5°C.

Overall, the subsurface anomalies throughout the equatorial Pacific were generally within ±1.5°C of their long-term mean. When it is considered that the previous year's subsurface temperatures reached +4°C by November (with a maximum local anomaly of +5.3°C) (Watkins 2003), and that in comparative terms the peak of the El Niño event in 1997-98 saw subsurface anomalies reach in excess of +8°C, spring 2003 was clearly neutral below the ocean surface as well as on and above it.

Surface analyses

The southern hemisphere spring 2003 MSLP pattern, computed from the Bureau of Meteorology's Global Assimilation and Prediction (GASP) model, is shown in Fig. 7, with the corresponding anomaly pattern provided in Fig. 8. These anomalies are the difference from a 22-year (1979-2000) climatology obtained from the National Centers for Environmental Prediction (NCEP) II Reanalysis data (Kanamitsu et al. 2002).

The spring MSLP pattern in Fig. 7 was largely zonal in structure, with arguably a wave number three pattern. Troughs were located at 30°E, 180ºE and 100ºW. As expected from climatology, the subtropical ridge and the Antarctic high were the dominant high pressure features, whilst the Antarctic circumpolar trough was the significant low pressure feature.

Fig. 6 Four month August to November 2003 sequence of vertical temperature anomalies at the equator. Contour interval is 0.5°C.

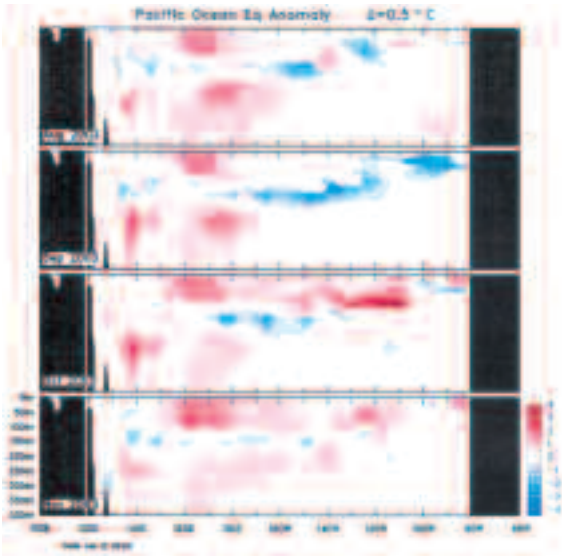

The MSLP anomaly distribution (Fig. 8) for spring 2002 shows several notable anomalies, with most at the mid to high latitudes – though this is to be expected owing to this region having the highest variability. Hence one could argue that normalised anomalies may indicate other regions which have greater deviations relative to their local variance.

In the tropical Pacific MSLP anomalies were small in magnitude (reaching a minimum of –1.9 hPa, compared with the previous year's spring values of down to –3.9 hPa), but nonetheless negative. This is not surprising given the continuation of weakly positive SST anomalies (Fig. 4), which would have enhanced low-level warming and hence reduced pressures.

MSLP anomalies at the mid latitudes were largely linked to changes at the high latitudes. The two regions with largest anomaly values occurred off the Amundsen and Bellingshausen Seas, with a positive anomaly of +7.5 hPa, and northeast of the Weddell Sea. In both cases, as well as for north of East Antarctica, the maximum MSLP positive anomaly occurred just to the north of the sea ice edge. This is not surprising, as in all three regions the sea-ice edge was further north than usual. Hence, as the region near the sea-ice edge during spring is often one of the first areas where cold divergent air encounters the 'warm' underlying ocean (and hence low-level warming/reduction in surface pressure), a movement of the

Fig. 7 Mean sea-level pressure for spring 2003 (hPa).

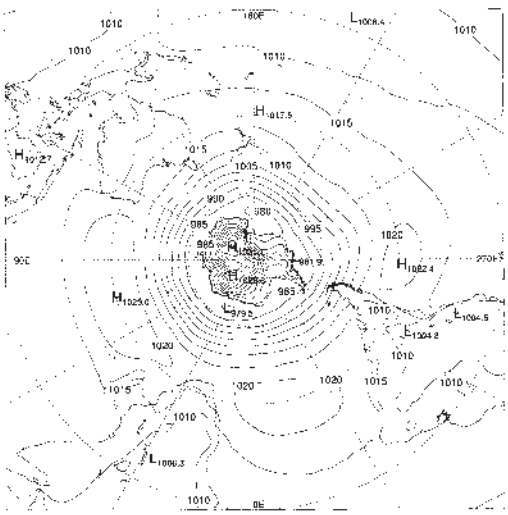

Fig. 8 Anomalies of the mean sea-level pressure from the 1979-2000 National Centers for Environmental Prediction reanalysis II climatology, for spring 2003 (hPa).

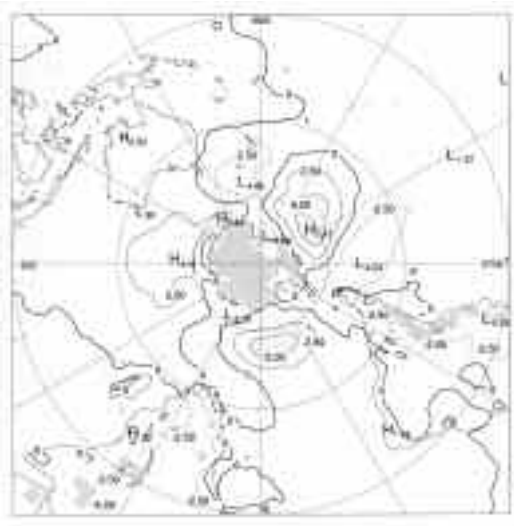

sea-ice edge north results in a shift in the location of this process (Watkins and Simmonds 1995), and thus higher than normal pressures.

Over Australia the MSLP was far higher than normal over virtually the entire continent, with the largest pressure anomalies occurring over northern Australia. The generally higher pressures reflected the increased OLR (decreased high cloud) observed during the season.

Mid-tropospheric analyses

The 500 hPa geopotential height (an indicator of the steering of surface synoptic systems) across the southern hemisphere is shown in Fig. 9, and anomalies in the 500 hPa field displayed in Fig. 10.

The analysis of the 500 hPa height shows a split in the flow in the Tasman Sea, as well as to the east of New Zealand/southern Pacific Ocean. A further split is apparent to the west of Western Australia. These splits reflect slightly lower pressures at the surface, associated with blocking systems in these regions (Fig. 8). This is discussed further in the following section.

At the mid to high latitudes, the major 500 hPa height anomalies were centred over the same locations as their MSLP counterparts. Combined, this suggests a largely barotropic atmospheric structure.

Blocking

The time-longitude section of the daily southern hemisphere Blocking Index (BI)* is shown in Fig. 11. This index is a measure of the strength of the zonal 500 hPa flow in mid latitudes relative to that at subtropical and high latitudes. Positive values of the blocking index are generally associated with a split in the mid-latitude westerly flow centred near 45°S and mid-latitude blocking activity.

The BI values during spring 2003 showed several relatively strong blocking events (BI > 60). The first event occurred in early September, with the block centred on the date-line and lasting for the first 10 days of the month. Further blocking occurred in this region in the first week of October, whilst it was not until mid- to late November that the final block of the season occurred in the Pacific sector. The region from eastern Australia to the central Pacific (140ºE to 220°E/140ºW) is climatologically favoured for blocking (Trenberth and Mo 1985, Sinclair 1996). As shown in Fig. 9, this region was the most notable region of split flow at the 500 hPa level.

Elsewhere, the only other strong block occurred in the eastern Indian Ocean, off Western Australia, in late September.

The seasonal mean blocking index is shown in Fig. 12. Mean positive values occurred between 160°E

*$BI = 0.5[U_{25} + U_{30} - (U_{40} + 2U_{45} + U_{50}) + U_{55} + U_{60}]$ where U_{xx} is the westerly component of the 500hPa wind at latitude xx.

Fig. 9 Mean 500 hPa geopotential heights for spring 2003 (gpm).

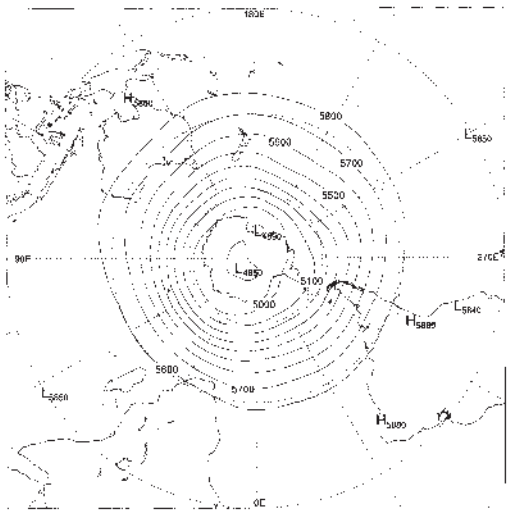

Fig. 10 Anomalies of the 500 hPa geopotential height from the 1979-2000 National Centers for Environmental Prediction reanalysis II climatology, for spring 2003 (gpm).

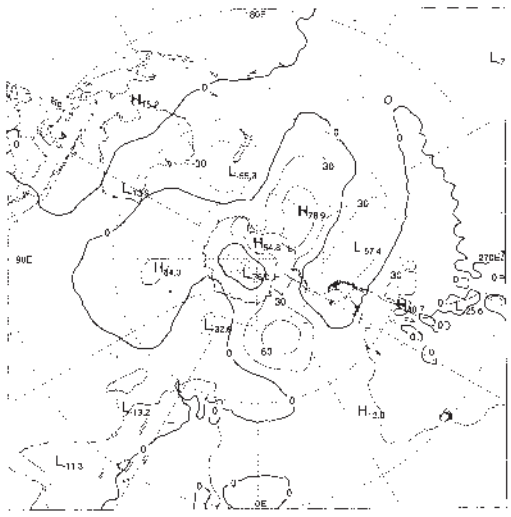

and 250°E/110°W, an eastwards shift from the climatological mean positive BI region: 150°E to 120°W. Observed values were greater, however, than climatological values in the eastern Pacific, the Atlantic and in the eastern Indian oceans, the latter region being offshore of Western Australia.

Fig. 11 Spring 2003 daily blocking index: time-longitude section. Day 1 is 1 September.

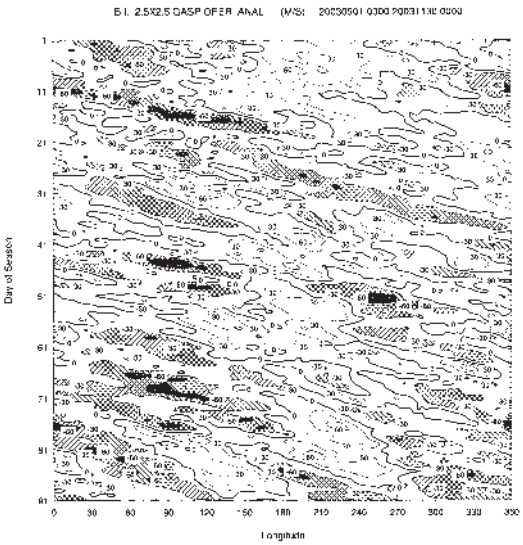

Anticyclonicity (taken as the time in hours anticyclones spend in any 5° x 5° sector (Nowak and Leighton (1997)) maps for spring 2003 (not shown) indicate positive anticyclonicity anomalies in the Great Australian Bight, as well as in the region of blocking off the Western Australian coast.

Winds

Spring 2003 low-level (850 hPa) and upper level (200 hPa) wind anomalies (from the 22 year NCEP II climatology) are shown in Figs 13 and 14 respectively.

At the low levels the wind anomalies generally reflected the MSLP anomalies (Fig. 8). Largest anomalies tended to occur in the mid to high latitudes. Largest anomalies occurred in the Pacific sector in the vicinity of 60°S, 100°W, with southeasterly anomalies of up to 5.8 m s^{-1}. Interestingly much of the Pacific sector of the Southern Ocean showed anomalously strong winds, whilst the Indian Ocean and to a lesser extent the Atlantic, displayed relatively small anomalies.

In the tropical Pacific, low-level winds (and hence the trade winds) were near normal, reflecting the generally neutral ENSO conditions. Closer to the South American coast, however, the trades south of the equator were enhanced, thereby encouraging the ocean surface flow away from the landmass, thus increasing the upwelling of cooler deep waters. The associated cooling at the surface is apparent in Fig. 4. North of the equator in the far eastern tropical Pacific,

Fig. 12 **Mean southern hemisphere blocking index for spring 2003 (bold line). The dashed line shows the corresponding long-term average. The horizontal axis shows the degrees east of the Greenwich meridian.**

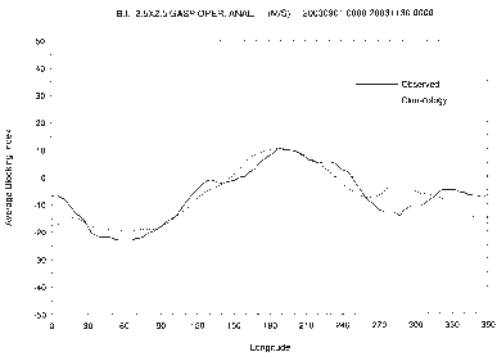

anomalous westerlies were apparent, possibly associated with a northwards shift in the intertropical convergence zone (ITCZ).

The upper-level wind anomalies (Fig. 14) in the tropical Pacific were also close to normal in the central and western regions. Closer to the South American coast, however, westerly flow was enhanced. This circulation corresponds to what may have been expected given the low level easterly anomalies.

In the Australian region the low-level wind anomalies were generally small. Over the continent, northwesterly anomalies were apparent across the centre and through Western Australia, associated with the higher MSLP observed over the Top End. Most interesting, however, was the easterly anomalies along the southern fringes of the continent and offshore, suggesting a reduction in the strength, or possible southwards shift, in the westerlies. This shift south is somewhat supported by the anticyclonicity maps of Leighton (not shown), which suggest high pressure systems tended to remain further south than the long-term mean through the Great Australian Bight. Individual monthly wind anomalies (not shown) suggest that strongest easterly anomalies were experienced during October, when significantly higher than normal MSLP was observed to the south and southwest of the continent, whilst in November, anomalously high pressure over the Bight and to its south also contributed to a slight reduction in the strength of the westerlies. The reduction in the westerlies during spring was in contrast to winter 2003, when westerly anomalies were observed over the same regions (Dawkins 2004).

Ozone hole observations

The Austral spring is typically the time of the maximum extent of the Antarctic ozone hole, as well as the time of lowest annual ozone levels. In the absence of sunlight, the wintertime polar vortex in the lower

Fig. 13 **Spring 2003 850 hPa vector wind anomalies with contours of vector magnitude overlayed. The contour interval is 5 m s^{-1}, with values above 5 m s^{-1} stippled.**

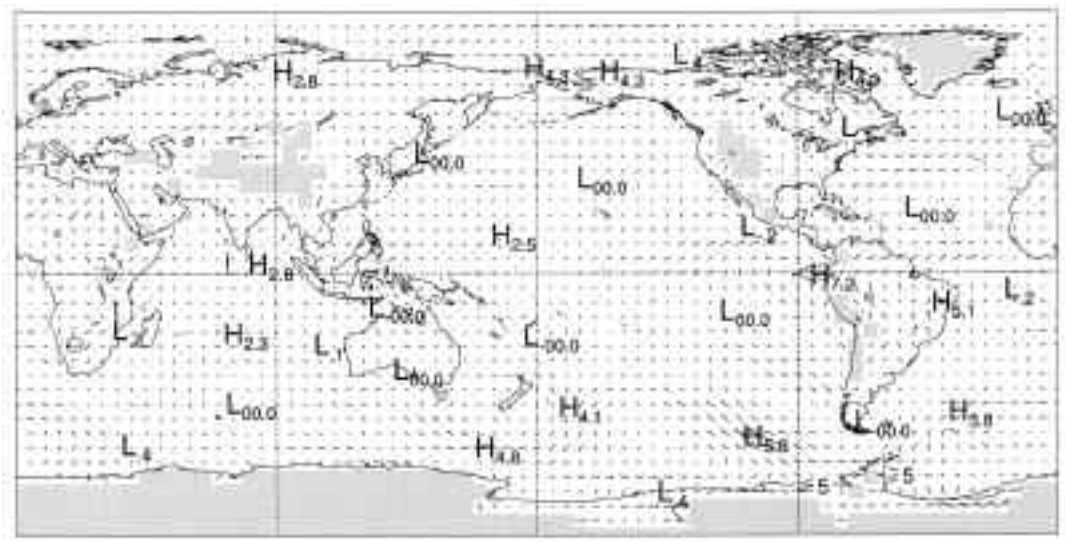

Fig. 14 Spring 2003 200 hPa vector wind anomalies with contours of vector magnitude overlayed. The contour interval is 5 m s^{-1}, with values above 5 m s^{-1} stippled.

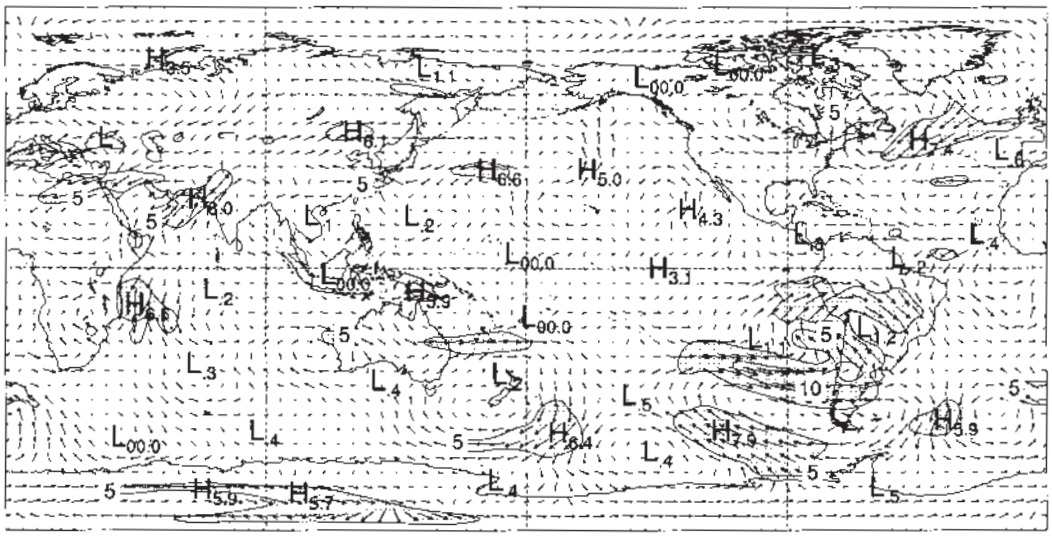

stratosphere cools to below –78ºC enabling polar stratospheric ice clouds to form. Chlorine and bromine compounds react in the ice clouds to produce chemical species that, when combined with the incoming UV radiation as the sunlight returns in spring, destroy ozone (WMO 1998). As the stratosphere warms in spring (and hence ice clouds can no longer form) this process weakens. Ozone levels then return to near normal by early summer. The compounds that lead to the ozone breakdown are largely anthropogenic, but now appear to be in decline (WMO 1998).

Figure 15 shows the mean ozone measurements for spring 2003 from the Total Ozone Mapping Spectrometer (TOMS) instruments. Typically, the ozone hole is taken as the area of total column ozone with a value of less than 220 Dobson units.

By August 2002 conditions in the stratosphere were primed for a large ozone hole. Temperatures in the lower stratosphere within the polar vortex were at the low end of the range measured during the previous twenty years; temperatures as low as –100°C were reached briefly in early August. By mid September, this outlook proved correct, with the ozone hole reaching 28 million km^2. A brief decrease in size occurred, but then the hole expanded once more and again reached 28 million km^2 in late September, having varied between 25 and 28 million km^2 throughout the month. This peak area is comparable to the record ozone hole observed in 2000 (28.5 million km^2 (Watkins 2000)), and far exceeds the 1991-2002 mean peak value of over 21 million km^2. Of some concern was the area of ozone values which were 50 per cent below their pre-ozone hole norms (i.e. ozone values during the period 1964-76). This 50 per cent area reached 15 million km^2 for the first time in recorded history, eventually peaking on September 26 at 18 million km^2. The 50 per cent area had only breached 10 million km^2 four times previously.

By the second week of October, the ozone hole had reduced to 18 million km^2, with a rapid reduction in size until its disappearance in mid-November (in 2000 the hole did not dissipate until mid-December). Overall, the peak ozone hole size was not only comparable to the 2000 record, but was also some 9 million km^2 larger than the ozone hole of the previous year, when the ozone hole effectively split in two in late September (Watkins 2003).

In further contrast to 2002, the ozone hole was far deeper in 2003, reaching a minimum total column ozone of around 100 Dobson Units (DU) in late September/early October, considerably less than the 2002 value of 135 DU, but thankfully more than the record satellite observation of 88 DU in 1994.

The return to near record ozone values in 2003 highlights the comments made in the previous year (WMO 2002) that the relatively weak nature of the 2002 ozone hole was a result of anomalous circulation and meteorological conditions associated with the polar vortex and not an indication of a return to a normal chemical composition of the stratosphere.

Fig. 15 Total column ozone values from the Total Ozone Mapping Spectrometer (TOMS) for spring 2003 (Dobson Units).

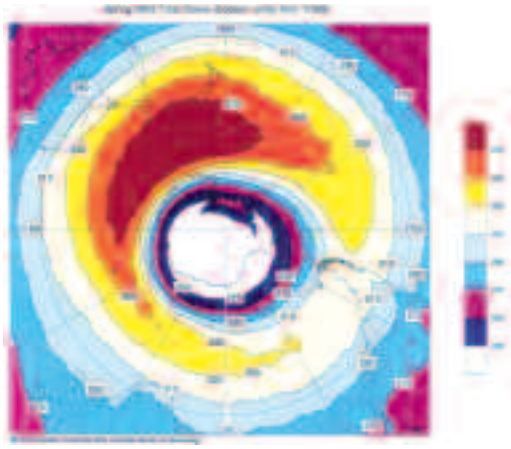

Australian region

Rainfall

The distribution of Australian rainfall totals for spring 2003 is shown in Fig. 16, whilst Fig. 17 shows the associated decile ranges based on gridded rainfall data for all springs from 1900 to 2003.

Highest rainfall totals for the season were recorded in western Tasmania, where in excess of 400 mm fell for the season. For the remainder of the states precipitation in excess of 200 mm occurred over the Australian Alps, in several places along the Great Dividing Range in New South Wales, along the south-western tip of Western Australia and in the Kimberly. In contrast, far north Queensland (including Cape York Peninsula), as well as western Queensland, the eastern Northern Territory and western central Western Australia all had large areas which received less than 25 mm of rainfall. Inland from Normanton (Queensland) and along the Western Australian coast around Port Hedland, less than 2 mm was recorded for the season.

Despite the neutral atmospheric and oceanic conditions in the tropical Pacific, rainfall totals were drier than normal through much of Queensland during the season. A non-trivial portion of that State received very much below average rainfall (i.e. rainfall within the lowest 10 per cent of spring totals recorded; Fig. 17), whilst a small area of Cape York Peninsula received its lowest rainfall on record. Overall it was Queensland's 11th driest spring on record. Elsewhere, the Northern Territory also received below normal rainfall in a number of areas.

In contrast, Western Australia was generally wetter then normal, with much of the southern and eastern halves of the state receiving above average rainfall and relatively large expanses recording rainfall within the highest 10 per cent of recorded totals. Despite the generally wetter than normal conditions in Western Australia, it only managed to record its 17th wettest spring on record with an average precipitation of 57.4 mm, well below the record 110.5 mm recorded in 1975.

Over the remainder of the continent, conditions were generally closer to average. Unfortunately for many, this included the catchments for the three main population centres experiencing water deficiencies; Perth, Melbourne and Sydney. As La Niña events follow El Niño events around 40 to 45 per cent of the time, the eastern States, at least, would have been hoping for conditions climatologically favourable for above average rainfall. The return to only near normal rainfall, at best, whilst far better than the drought conditions being experienced at the same time in the previous year, meant a prolonged recovery from arguably one of the worst droughts in modern Australia's history (Nicholls 2004).

The seasonal pattern of drier than normal in the northeast quarter of the continent and wetter than normal in the west was arguably the result of similar patterns in both September and November. Wet conditions over inland and southern coastal Western Australia during September were followed up by decile 10 rainfall (i.e. rainfall totals in the highest 10 per cent of historical observations) over a large portion of inland Western Australia during November. The end result was Western Australia's eighth wettest November on record (records commenced 1900). In contrast, New South Wales, eastern South Australia and Queensland all experienced significant areas of decile 1 rainfall (i.e. rainfall totals in the lowest 10 per cent of historical observations) during September. For New South Wales, it was its fifth driest, and for Queensland it's seventh driest, September on record. Whilst parts of these regions received above normal rainfall in October (and in New South Wales, November also), Queensland again suffered below average rainfall in November with large areas of decile 1 rainfall once more.

The other State to be severely impacted during November was Tasmania, which recorded its lowest November rainfall on record (104 years), with a Statewide average rainfall of only 23.5 mm for the month, significantly below the previous lowest record set in November 1900 of 29.6 mm and the 1961-90 November average of 87.4 mm.

Fig. 16 Rainfall totals over Australia for spring 2003 (mm).

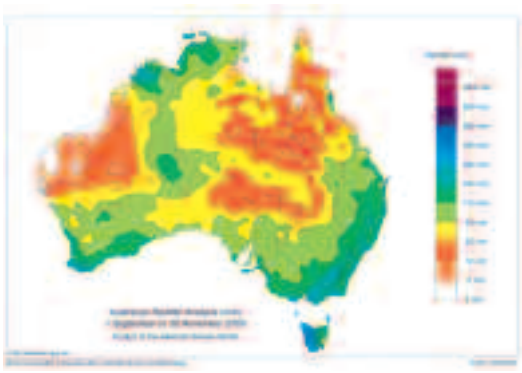

Fig. 17 Spring 2003 rainfall deciles for Australia: decile range based on grid-point values over the spring periods from 1900 to 2003.

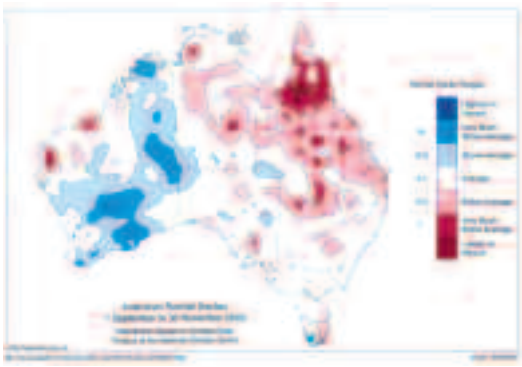

Overall, spring 2003 was ranked 40 out of the 104 years of Australia-wide records (i.e. 40th driest), with a mean rainfall of 60 mm. Whilst it would clearly have been preferable for the continent to have received rainfall in the upper half of historical records, it was still a considerable improvement from the previous year's spring (Watkins 2003), which was the fifth driest on record with an Australia-wide mean rainfall of only 37.9 mm. Spring 2003 saw 60 per cent of the area of the continent experience rainfall below the long-term median, though only 5 per cent of the continent was in decile 1 (in contrast, for spring 2002 the area was 26 per cent).

Table 1 summarises the seasonal rainfall extremes and rankings on a national and State basis.

Temperatures

The spring 2003 mean maximum and minimum temperature anomalies, calculated with respect to the reference period 1961-90, are shown in Figs 18 and 19 respectively. The Australia-wide mean maximum temperature anomaly (relative to the 1961-90 mean) for spring 2003 was +0.53°C; the 15th warmest spring maximum in the high quality Australian record (data since 1950). Similarly the Australia-wide minimum spring temperature anomaly was +0.30°C.

Over the eastern half of the continent the maximum temperature anomalies generally displayed a negative correlation with the rainfall totals, with anomalies of greater than +1°C over most regions which received below normal rainfall (i.e., Queensland and the Northern Territory). In Queensland, large parts of the far north (where rainfall was lowest on record or in decile 1) experienced decile 10 maximum temperatures (with highest on record seasonal temperatures in an area near Mackay), resulting in Queensland as a whole having its fifth warmest (out of 54 years of high quality State-wide monitoring) spring on record, with a State-wide anomaly of +1.2°C.

In regions with closer to average rainfall through Victoria and southern coastal Australia, cooler than normal maximum temperatures were present, including a number of areas with anomalies below –1°C. These cooler than normal maximum temperatures may have been the result of the southwards shift in the subtropical ridge feeding air from further south into the region. Over Victoria and Tasmania (the only states or territories to record negative state-wide anomalies) cyclonic MSLP anomalies centred over southern New Zealand (Fig. 8) suggested some enhanced southerly component to the flow (Fig. 13) over these two States. This increased southerly component was most apparent in October and November (not shown), the result of lower pressures than normal (anomalies of –2 hPa) in the Tasman Sea during October, and higher pressures than normal west of Tasmania (anomalies of up to +5 hPa) during November.

Minimum temperature anomalies displayed some similarities to the maximum temperature anomalies, which for far north Queensland might be somewhat unexpected given the generally positive OLR anomalies (not shown) in the region, and hence an expectation of less night-time cloud. However given that during spring the amounts of high cloud in these regions are climatologically low, the OLR anomalies may be more a reflection of the intense daytime surface heating rather than a true reduction in cloud amount, and hence cloud at night may have been insignificantly different from normal.

Table 1. Rainfall.

	Highest seasonal total (mm)	*Lowest seasonal total (mm)*	*Highest 24 hour fall (mm)*	*area-averaged rainfall (AAR) (mm)*	*rank of AAR **
Australia	978 at Strathgordon (TAS)	Zero at several locations (QLD and WA)	121 at Dungog (NSW) on 24 November	60	40
WA	446 at Walpole	Zero at several locations	85 at Woogenellup on 30 September	56	88
NT	359 at Ludmilla	3 at Ammaroo	92 at Ludmilla on 17 November	50	42
SA	301 at Piccadilly	3 at Moomba	52 at Bimbowrie on 1 October	47	54
QLD	437 at Bellenden Ker Top Station	Zero at several locations	115 at Waterloo on 24 November	39	11
NSW	509 at Thredbo Village	5 at Barrona Downs	121 at Dungog on 24 November	102	41
VIC	576 at Rocky Valley	44 at Kyndalyn Park	82 at Bullengarook East on 23 November	158	40
TAS	978 at Strathgordon	55 at Triabunna	65 at Mt Read on 17 September	301	52

* The rank goes from 1 (lowest) to 104 (highest) and is calculated on the years 1900 to 2003 inclusive.

Fig. 18 Spring 2003 maximum temperature anomalies for Australia based on a 1961-90 mean (°C).

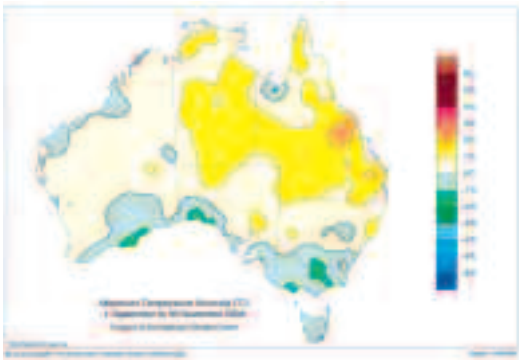

Fig. 19 Spring 2003 minimum temperature anomalies for Australia based on a 1961-90 mean (°C).

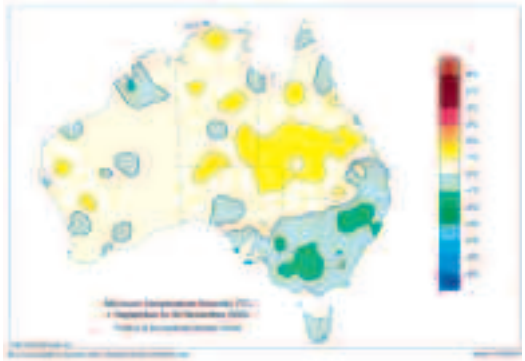

Minimum temperature anomalies of greater than +1°C extended through central Queensland and into parts of the Northern Territory. Anomalies below –1°C occurred over northeastern New South Wales and central and northern Victoria/southern New South Wales. Over the Great Dividing Range and Alpine regions of Victoria, minimum temperatures were generally in the lowest 10 per cent of recorded values. This contributed to the Victoria State-wide average for spring being 0.93°C below normal, the third lowest (out of 54 years) mean minimum temperature on record. Similarly, Tasmania recorded its seventh lowest mean minimum temperature on record and the largest negative anomaly since 1970. In general, most of southeastern Australia experienced below average minimum temperatures during spring.

Table 2 summarises the seasonal maximum temperature ranks and extremes on a national and state basis, whilst Table 3 gives the corresponding summary for the seasonal minimum temperatures.

References

Beard, G.S. 2004. Seasonal climate summary southern hemisphere (autumn 2003): demise of the 2002/03 El Niño event. *Aust. Met. Mag., 53*, 53-63.

Climate Prediction Center. 2003. *Climate Diagnostics Bulletin*, September, October, November 2003. US Department of Commerce, National Oceanic and Atmospheric Administration, Washington D.C.

Dawkins, S.S. 2004. Seasonal climate summary southern hemisphere (winter 2003): a warm season with an exceptionally wet August. *Aust. Met. Mag., 53*, 133-43.

Table 2. Maximum temperature.

	Highest seasonal mean (°C)	*Lowest seasonal mean (°C)*	*Highest daily recording (°C)*	*Lowest daily recording (°C)*	*Anomaly of area-averaged mean (°C) (AAM)*	*Rank of AAM **
Australia	39.3 at Wyndham (WA)	5.5 at Mt Hotham (VIC)	46.0 at Windorah (QLD) on 19th November	–4.1 at Mt Hotham (VIC) on 14th September	+0.53	39
WA	39.3 at Wyndham	18.2 at Albany	45.2 at Mandora on 9 November, at Eneabba on 11 November and at Marble Bar on 30 November	10.9 at Manjimup on 10 September	+0.09	28
NT	38.6 at Bradshaw	31.0 at Kulgera	44.5 at Ngukurr on 29 October	16.9 at Kulgera on 16 September	+0.89	45
SA	31.0 at Oodnadatta	14.1 at Mt Lofty	44.0 at Marree on 16 November	5.7 at Mount Lofty on 14 September	+0.42	33
QLD	37.2 at Julia Creek	22.4 at Stanthorpe	46.0 at Windorah on 19 November	14.0 at Stanthorpe on 2 September	+1.23	50
NSW	29.4 at Mungindi	6.1 at Crackenback	43.3 at Bourke on 20 November	–4.0 at Crackenback on 14 September	+0.28	37
VIC	24.0 at Mildura	5.5 at Mt Hotham	41.6 at Ouyen on 15 November	–4.1 at Mt Hotham on 14 September	–0.48	20
TAS	17.5 at Swansea	6.4 at Mt Wellington	34.1 at Friendly Beaches on 15 November	–1.7 at Mount Wellington on 10 October	–0.40	19

* The temperature ranks go from 1 (lowest) to 54 (highest) and are calculated on the years 1950 to 2003 inclusive.

Table 3. Minimum temperature.

	Highest seasonal mean (°C)	*Lowest seasonal mean (°C)*	*Highest daily recording (°C)*	*Lowest daily recording (°C)*	*Anomaly of area-averaged mean (°C) (AAM)*	*Rank of AAM **
Australia	26.2 at Troughton Island (WA)	–1.2 at Crackenback (NSW)	32.0 at Boulia (QLD) on 19 November	–15.0 at Charlotte Pass (NSW) on 28 September	+0.30	38
WA	26.2 at Troughton Island	7.2 at Wandering	31.0 at Warmun on 2 November	–2.2 at Eyre on 29 October	+0.28	35
NT	25.2 at Warruwi	14.5 at Alice Springs	30.9 at Jervois on 28 October	–0.5 at Alice Springs on 3 September	+0.33	33
SA	15.5 at Moomba	5.9 at Keith	28.7 at Moomba on 18 November	–3.2 at Yongala on 28 September	+0.63	43
QLD	24.7 at Sweers Island	7.7 at Stanthorpe	32.0 at Boulia on 19 November	–3.5 at Oakey on 3 September	+0.61	45
NSW	16.1 at Cape Byron	–1.2 at Crackenback	29.5 at Tibooburra on 20 November	–15.0 at Charlotte Pass on 28 September	–0.38	18
VIC	10.7 at Gabo Island	–0.7 at Mt Hotham	23.5 at Mildura on 30 November	–9.2 at Mt Hotham on 28 September	–0.93	3
TAS	9.3 at Swan Island	–1.0 at Mount Wellington	20.4 at Strahan on 30 November	–10.7 at Liawenee on 8 September	–0.71	7

Hoerling, M.P., Kumar, A. and Zhong, M. 1997. El Niño, La Niña, and the nonlinearity of their teleconnections. *J.Clim., 10,* 1769-86.

Kanamitsu, M., Ebisuzaki, W., Woollen, J., Yang, S.-K., Hnilo, J.J., Fiorino, M. and Potter, G.L. 2002. NCEP-DOE AMIP-II Reanalysis (R-2). *Bull. Am. Met. Soc., 83,* 1631-43.

Kwok, R. and Comiso, J.C. 2002. Southern Ocean climate and sea ice anomalies associated with the Southern Oscillation. *J. Clim., 15*, 487-501.

Madden, R.A. and Julian, P.R. 1971. Detection of a 40-50 day oscillation in the zonal wind in the tropical Pacific. *J. Atmos. Sci., 28*, 702-708.

Madden, R.A. and Julian, P.R. 1972. Description of global scale circulation cells in the tropics with a 40-50 day period. J. *Atmos. Sci., 29*, 1109-23.

National Climatic Data Center (NCDC) 2004. http://www.ncdc.noaa.gov/oa/climate/research/monitoring.html

Nicholls, N. 2004. The changing nature of Australian droughts. *Climatic Change, 63*, 323-36.

Nowak, H. and Leighton, R.M. 1997. Relationships between east coast Australasian anticylonicity, the Southern Oscillation and Australian Rainfall. *Aust. Met. Mag., 46*, 267-76.

Sinclair, M.R. 1996. A climatology of anticyclones and blocking for the Southern Hemisphere. *Mon. Weath. Rev., 124,* 245-63.

Trenberth, K. and Mo, K.C. 1985. Blocking in the Southern Hemisphere. *Mon. Weath. Rev., 113*, 3-21.

Vincent, D.G. 1993. The South Pacific Convergence Zone (SPCZ): A review. *Mon. Weath. Rev., 122,* 1949-70.

Vincent D.G., Fink, A., Schrage, J.M. and Speth, P. 1998. High- and low-frequency intraseasonal variance of OLR on annual and ENSO timescales. *J. Clim., 11*, 968-86.

Watkins, A.B. 2000. Seasonal climate summary southern hemisphere (spring 2000): a third successive positive phase of the Southern Oscillation begins. *Aust. Met. Mag., 50*, 295-308.

Watkins, A.B. 2003. Seasonal climate summary southern hemisphere (spring 2002): the El Niño reaches maturity and dry conditions dominate Australia. *Aust. Met. Mag., 52*, 213-26.

Watkins, A.B. and Simmonds, I. 1995. Sensitivity of numerical prognoses to Antarctic sea ice distribution. *J. Geophys. Res., 100*, 22681-96.

Watkins, A.B. and Simmonds, I. 1999. A late spring surge in the open water of the Antarctic sea ice pack. *Geophys. Res. Lett., 26*, 1481-4.

Wolter, K. and Timlin, M.S. 1993. Monitoring ENSO in COADS with a seasonally adjusted principal component index. *Proc. of the 17th Climate Diagnostics Workshop*, Norman, OK, NOAA/NMC/CAC, NSSL, Oklahoma Clim. Survey, CIMMS and the School of Meteor., Univ. of Oklahoma, 52-57.

Wolter, K., and Timlin, M. S. 1998. Measuring the strength of ENSO - how does 1997/98 rank? *Weather, 53*, 315-24.

World Meteorological Organization (WMO). 1998. Scientific assessment of ozone depletion: 1998. *Global Ozone Research and Monitoring Project Report No. 44*, WMO, Geneva. 500pp.

World Meteorological Organization (WMO) 2002. WMO Antarctic Ozone Bulletins. [Available from: http://www.wmo.ch/web/arep/gawozobull03.html]

Yuan, X. and Martinson, D.G. 2001. The Antarctic Dipole and its predictability. *Geophys. Res. Lett., 18*, 3609-12.

Appendix

The main sources for data used in this review were: National Climate Centre, *Climate Monitoring Bulletin - Australia*. Obtainable from: National Climate Centre, Bureau of Meteorology, GPO Box 1289K, Melbourne, Vic., 3001, Australia.

Climate Prediction Center, *Climate Diagnostics Bulletin*. Obtainable from: Climate Prediction Center, National Weather Service, Washington D.C., USA, 20233.

World Meteorological Organization, *Antarctic Ozone Bulletin*. Obtainable from: http://www.wmo.ch/web/arep/gawozobull03.html